LINEAR AND NON-LINEAR OSCILLATIONS IN MECHANICS

J H. Argyris, P.C. Dunne, T. Angelopoulos and B. Bichat
Imperial College of Science and Technology, University of London, England
Institut für Statik und Dynamik der Luft- und Raumfahrtkonstruktionen, Universität Stuttgart, West Germany

Abstract

This paper describes applications of some high order algorithms originally developed for structural dynamics to this and other problems. In the linear case the large step unconditionally stable algorithms are a useful alternative to modal analysis. For the accurate calculation of impulsive and wave like response small step methods are essential and these algorithms are also very suitable for non-linear problems. Illustrative examples from vibrations, flutter, non-linear wave propagation and the n-body problem are given.

1. Introduction

Most algorithms in common use for structural dynamics applications use low order explicit or implicit interpolation (1). In the algorithms described here (2) (3) (4) the inertia force is interpolated as a Hermitian polynomial in the time of degree 3, 5 or 7. Thus the 5th degree polynomial, for example, interpolates the inertia force $\boldsymbol{R}$ in terms of $\boldsymbol{R}_0, \dot{\boldsymbol{R}}_0, \ddot{\boldsymbol{R}}_0$ and $\boldsymbol{R}_1, \dot{\boldsymbol{R}}_1, \ddot{\boldsymbol{R}}_1$ at the beginning and end of a time interval t_0 to t_1. Two versions of the algorithm are used. In the first, which has a rather better truncation error, the velocity $\dot{\boldsymbol{r}}$ and displacement $\boldsymbol{r}$ are obtained from successive integrations of the acceleration using the interpolation polynomial and its first integral. In the second the same integration is used to obtain the displacement from $\dot{\boldsymbol{r}}$, $\boldsymbol{R}$ and $\dot{\boldsymbol{R}}$ as to obtain the velocity from $\boldsymbol{R}, \dot{\boldsymbol{R}}$ and $\ddot{\boldsymbol{R}}$. This results in an algorithm which is unconditionally stable for all integration time steps when applied to a linear oscillator (3).

The first, or small step algorithm, is recommended for impulsive load and wave problems and also for non-linear problems. The second or large step algorithm is an excellent alternative for modal analysis in linear systems and is still applicable with arbitrary damping.

The properties of the algorithms are summarised in TABLE 1 and 2. In TABLE 3 and Fig. 1 are given the period elongations for the large step algorithms which have no amplitude error for any time step. For comparison are given curves for the well known Newmark and Wilson (3) algorithms. The small step algorithms are a little more accurate for small steps but become unstable when the time step exceeds about half of the least period of the dynamic system.

		Coefficients of $\boldsymbol{M}^{-1}x$							
n		$\boldsymbol{R}_0$	$\boldsymbol{R}_1$	$\dot{\boldsymbol{R}}_0$	$\dot{\boldsymbol{R}}_1$	$\ddot{\boldsymbol{R}}_0$	$\ddot{\boldsymbol{R}}_1$	$\dddot{\boldsymbol{R}}_0$	$\dddot{\boldsymbol{R}}_1$
1	$\dot{\boldsymbol{r}}_1 = \dot{\boldsymbol{r}}_0 +$	$\frac{1}{2}\tau$	$\frac{1}{2}\tau$						
	$\boldsymbol{r}_1 = \boldsymbol{r}_0 + \tau\dot{\boldsymbol{r}}_0 +$	$\frac{1}{4}\tau^2$	$\frac{1}{4}\tau^2$						
2	$\dot{\boldsymbol{r}}_1 = \dot{\boldsymbol{r}}_0 +$	$\frac{1}{2}\tau$	$\frac{1}{2}\tau$	$\frac{1}{12}\tau^2$	$-\frac{1}{12}\tau^2$				
	$\boldsymbol{r}_1 = \boldsymbol{r}_0 + \tau\dot{\boldsymbol{r}}_0 +$	$\frac{1}{3}\tau^2$	$\frac{1}{6}\tau^2$	$\frac{1}{24}\tau^3$	$-\frac{1}{24}\tau^3$				
3	$\dot{\boldsymbol{r}}_1 = \dot{\boldsymbol{r}}_0 +$	$\frac{1}{2}\tau$	$\frac{1}{2}\tau$	$\frac{1}{10}\tau^2$	$-\frac{1}{10}\tau^2$	$\frac{1}{120}\tau^3$	$\frac{1}{120}\tau^3$		
	$\boldsymbol{r}_1 = \boldsymbol{r}_0 + \tau\dot{\boldsymbol{r}}_0 +$	$\frac{7}{20}\tau^2$	$\frac{3}{20}\tau^2$	$\frac{7}{120}\tau^3$	$-\frac{1}{24}\tau^3$	$\frac{1}{240}\tau^4$	$\frac{1}{240}\tau^4$		
4	$\dot{\boldsymbol{r}}_1 = \dot{\boldsymbol{r}}_0 +$	$\frac{1}{2}\tau$	$\frac{1}{2}\tau$	$\frac{3}{28}\tau^2$	$-\frac{3}{28}\tau^2$	$\frac{1}{84}\tau^3$	$\frac{1}{84}\tau^3$	$\frac{1}{1680}\tau^4$	$-\frac{1}{1680}\tau^4$
	$\boldsymbol{r}_1 = \boldsymbol{r}_0 + \tau\dot{\boldsymbol{r}}_0 +$	$\frac{5}{14}\tau^2$	$\frac{1}{7}\tau^2$	$\frac{11}{168}\tau^3$	$-\frac{1}{24}\tau^3$	$\frac{11}{1680}\tau^4$	$\frac{3}{560}\tau^4$	$\frac{1}{3600}\tau^5$	$-\frac{1}{3600}\tau^5$

TABLE 1 Family of Unconditionally Stable Algorithms for Linear Systems

		Coefficients of $M^{-1}x$							
n		R_0	R_1	$\dot{R}_0$	$\dot{R}_1$	$\ddot{R}_0$	$\ddot{R}_1$	$\dddot{R}_0$	$\dddot{R}_1$
1	$\dot{r}_1 = \dot{r}_0 +$	$\frac{1}{2}\tau$	$\frac{1}{2}\tau$						
	$r_1 = r_0 + \tau\dot{r}_0 +$	$\frac{1}{3}\tau^2$	$\frac{1}{6}\tau^2$						
2	$\dot{r}_1 = \dot{r}_0 +$	$\frac{1}{2}\tau$	$\frac{1}{2}\tau$	$\frac{1}{12}\tau^2$	$-\frac{1}{12}\tau^2$				
	$r_1 = r_0 + \tau\dot{r}_0 +$	$\frac{7}{20}\tau^2$	$\frac{3}{20}\tau^2$	$\frac{1}{20}\tau^3$	$-\frac{1}{30}\tau^3$				
3	$\dot{r}_1 = \dot{r}_0 +$	$\frac{1}{2}\tau$	$\frac{1}{2}\tau$	$\frac{1}{10}\tau^2$	$-\frac{1}{10}\tau^2$	$\frac{1}{120}\tau^3$	$\frac{1}{120}\tau^3$		
	$r_1 = r_0 + \tau\dot{r}_0 +$	$\frac{5}{14}\tau^2$	$\frac{1}{7}\tau^2$	$\frac{13}{210}\tau^3$	$-\frac{4}{105}\tau^3$	$\frac{1}{210}\tau^4$	$\frac{1}{280}\tau^4$		
4	$\dot{r}_1 = \dot{r}_0 +$	$\frac{1}{2}\tau$	$\frac{1}{2}\tau$	$\frac{3}{28}\tau^2$	$-\frac{3}{28}\tau^2$	$\frac{1}{84}\tau^3$	$\frac{1}{84}\tau^3$	$\frac{1}{1680}\tau^4$	$-\frac{1}{1680}\tau^4$
	$r_1 = r_0 + \tau\dot{r}_0 +$	$\frac{13}{36}\tau^2$	$\frac{5}{36}\tau^2$	$\frac{17}{252}\tau^3$	$-\frac{5}{126}\tau^3$	$\frac{1}{144}\tau^4$	$\frac{5}{1008}\tau^4$	$\frac{1}{3024}\tau^5$	$-\frac{1}{3780}\tau^5$

TABLE 2 Family of Conditionally Stable Algorithms for Linear and Non-Linear Systems

Order n	$\tan \Phi/2$	Period elongation	Period elongation for small $\omega\tau$	Φ for $\tau \to \infty$
1 (Newmark)	$\frac{1}{2}\omega\tau$	$\omega\tau/\Phi$	$1 + \frac{\omega^2\tau^2}{12}$	π
2	$\frac{1}{2}\omega\tau \Big/ \left(1 - \frac{1}{12}\omega^2\tau^2\right)$	"	$1 + \frac{\omega^4\tau^4}{720}$	2π
3	$\frac{1}{2}\omega\tau\left(1 - \frac{\omega^2\tau^2}{60}\right) \Big/ \left(1 - \frac{\omega^2\tau^2}{10}\right)$	"	$1 + \frac{\omega^6\tau^6}{100800}$	3π
4	$\frac{1}{2}\omega\tau\left(1 - \frac{\omega^2\tau^2}{42}\right) \Big/ \left(1 - \frac{3\omega^2\tau^2}{28} + \frac{\omega^4\tau^4}{1680}\right)$	"	$1 + O(\omega^8\tau^8)$	4π

TABLE 3 Summary of Properties of Matrix A where **A** is the operator

$$\begin{pmatrix} r_1 \\ \dot{r}_1 \end{pmatrix} = A \begin{pmatrix} r_0 \\ \dot{r}_0 \end{pmatrix}$$

see Ref. (3)

II. Application of Small Step Algorithms

Each time step is solved iteratively by Jacobi type iteration which is rapidly convergent for time steps very little shorter than those required for stability of the algorithm. It is unnecessary to form the complete stiffness matrix, indeed, even for linear systems it is better to avoid this when the system contains a very large number (over 600) degrees of freedom. Three possible flow charts are shown in Figs. 2,3 and 4 for linear and non-linear oscillations. For more details on these diagrams see (2). Some examples of the application of the small step algorithms are given in the following figures. They concern structural and non-structural examples. The achieved accuracy is in each case very satisfying. See also (2), (4), (5).

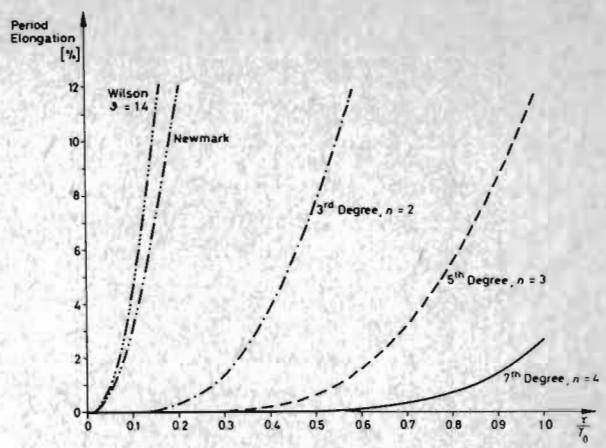

Fig 1 Percentage Period Elongation against (Time Step/Period). Comparison of the present algorithms with those of Wilson and Newmark.

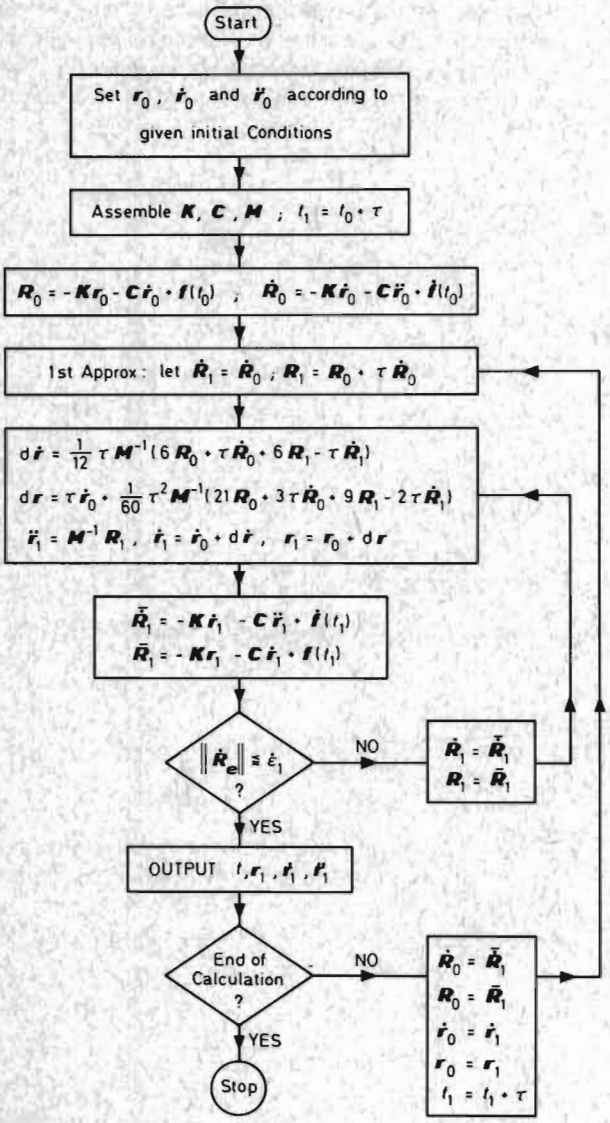

Fig 2 Flow Diagram for Linear Oscillation.Cubic Interpolation Small Step Algorithm.

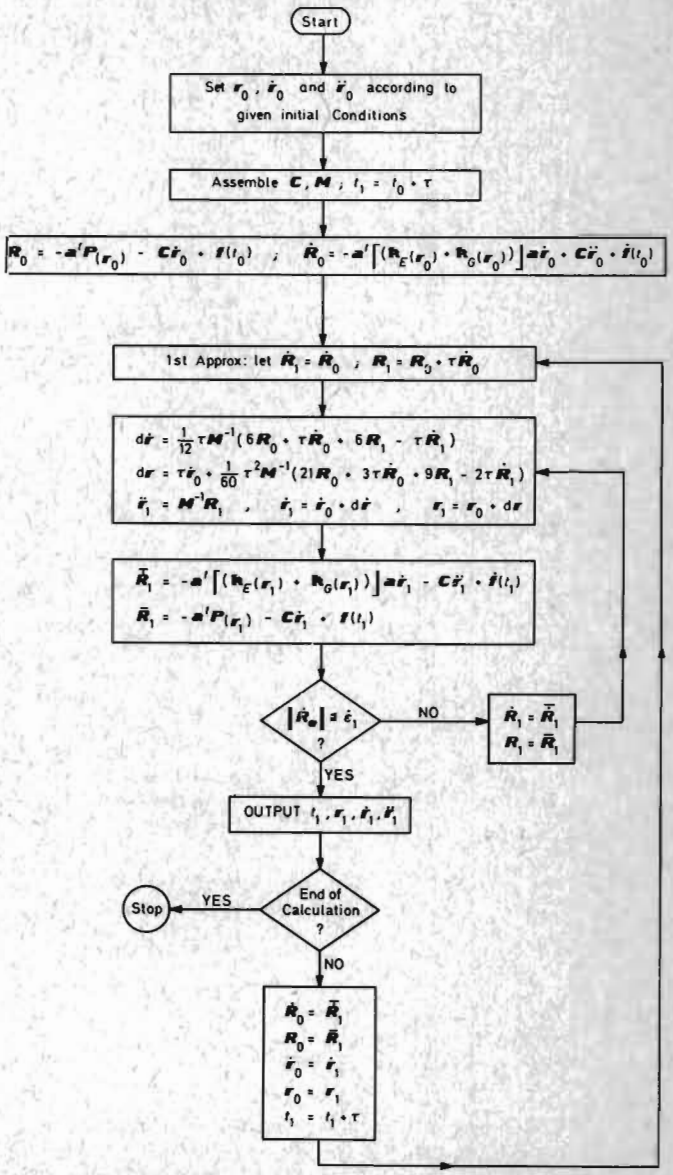

Fig 3 Flow Diagram for Non-Linear Oscillations.Cubic Interpolation. Small Step, not linearised

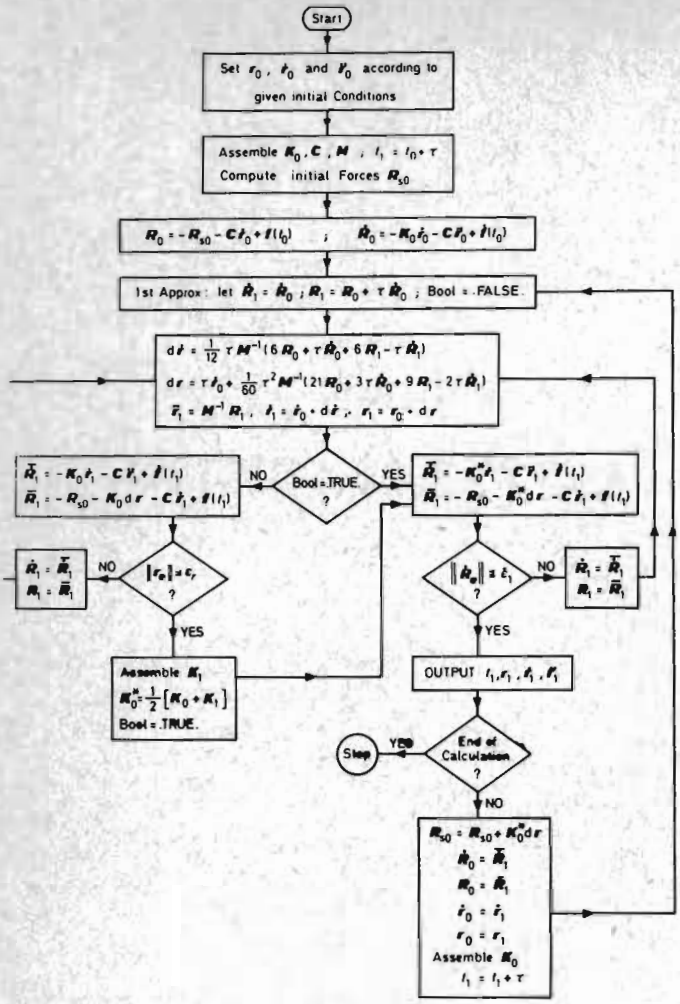

Fig 4 Flow Diagram for Non-Linear Oscillations

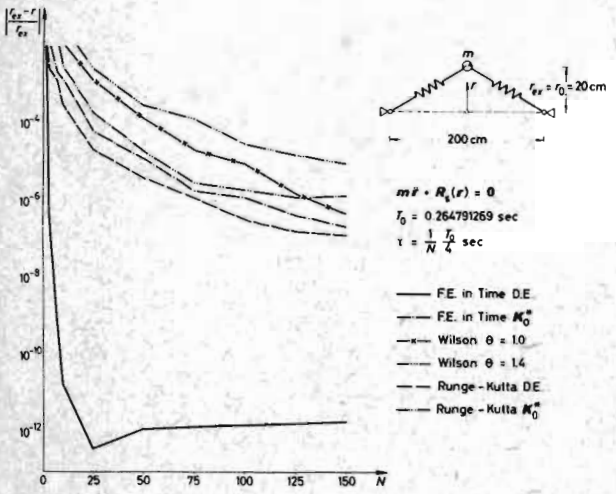

Fig 5 This example is a simple one degree of freedom system consisting of a prestressed weightless rod with a transversely vibrating mass at its centre. The graph shows the relative error for various methods in displacement as a function of the time step. See (2)

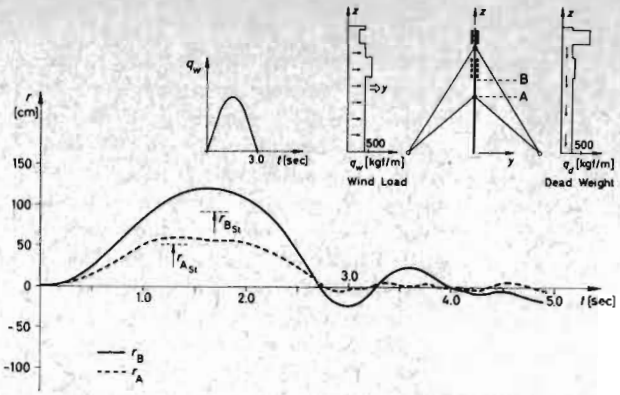

Fig 6 A transmitter tower of height 152.5 metres with triangular cross section space frame structure is supported by cables. It is analysed for wind load. There are 737 truss members and 549 degrees of freedom. As the bandwidth of the structural stiffness matrix is quite small the problem could be handled in core. The figure shows the displacements of two sections of the tower under transient wind loading. See (2)

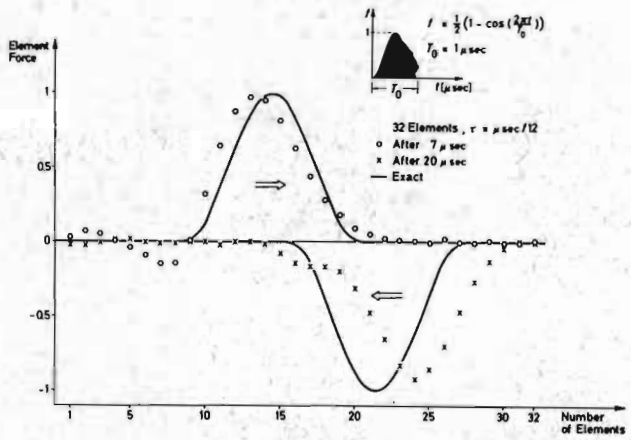

Fig 7 Cosine pulse through an elastic slab. See (1) and (2).

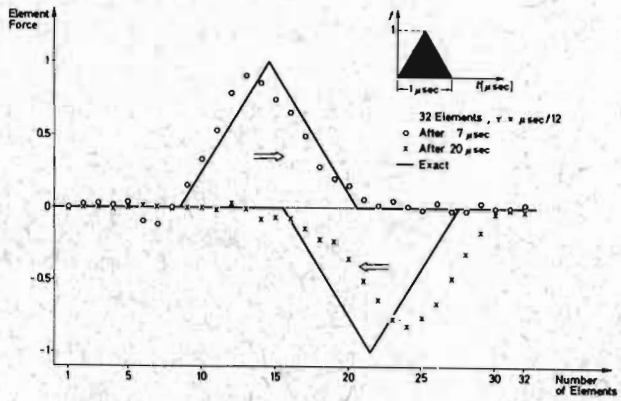

Fig 8 Triangular pulse through elastic slab. See (1) and (2)

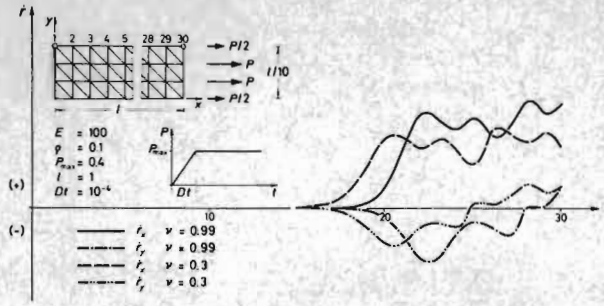

Fig 9 Non-linear material membrane under tensile step end load. The structure is idealised with 348 TRIM 3 finite elements. The calculations are made for two different values of Poisson's ratio and no damping is used. The graph shows the particle velocities of edge after 1 msec. The computation was made with the third degree algorithm.

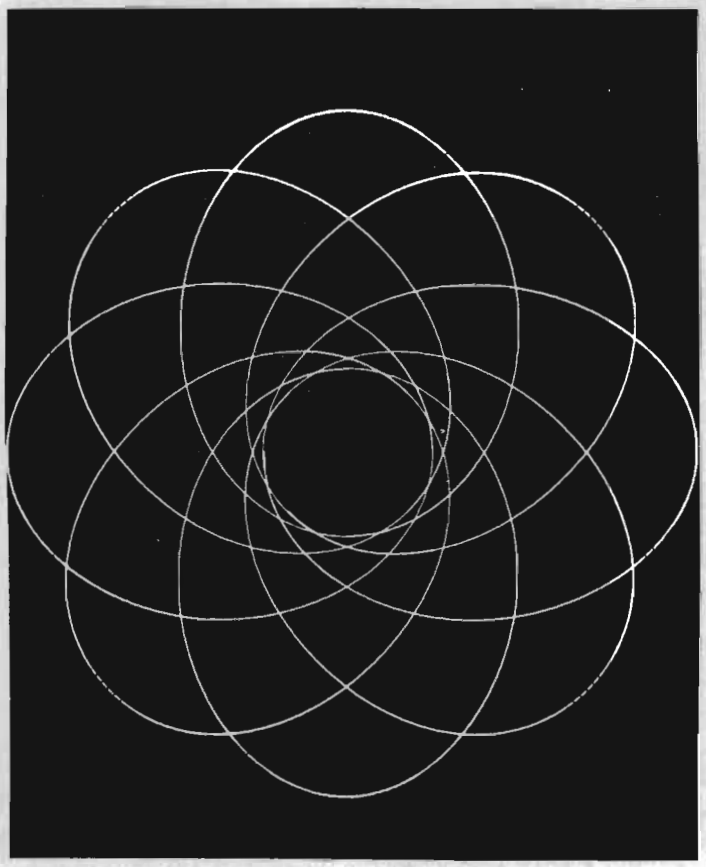

Fig. 10 N. Body problem. Eight equal masses turn around a central "sun" and influence each other simultaneously. The computation was realised with the fifth degree algorithm and appeared to be very exact. (See (4))

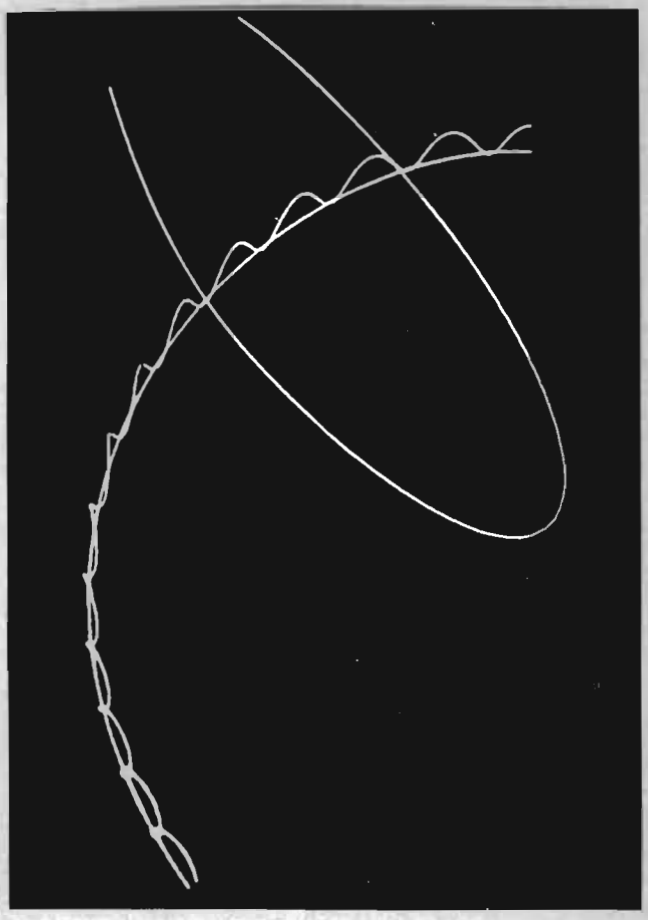

Fig 11 Other n.body problem. An earth turns around a central sun. A moon turns around the earth and a comet passes earth and sun. (See (4))

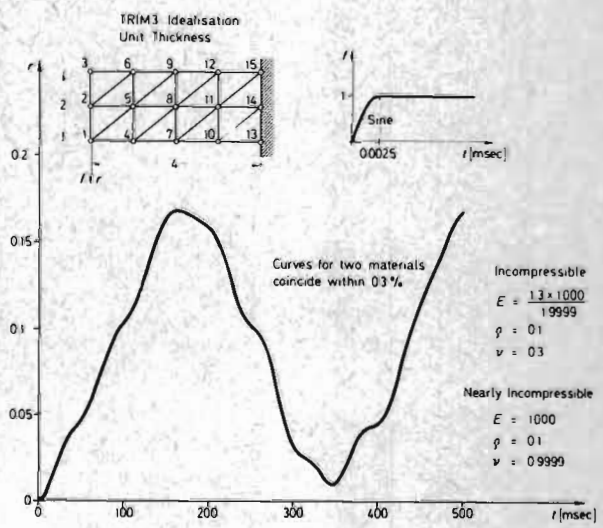

Fig 12 Dynamic response of cantilever beam with TRIM3 membrane idealisation. Incompressible ($\nu = 1.0$) and nearly incompressible ($\nu = 0.9999$). 24 nodal freedoms are reduced to 8 when the incompressibility constraint is applied. Third degree algorithm. See (5)

Fig 13 Supported bar of Mooney type material subject to a sinusoidal end loading. The data for the bar are found in (5). The load is of amplitude 50 units and period 2 msec with an initial tension cycle. The bar is represented by 60 lumped mass finite elements. In order to suppress high frequency oscillations a velocity damping matrix was assumed of 10^{-5} of the tangent stiffness matrix at the beginning of each step. The curves show the undamped and damped response at various times

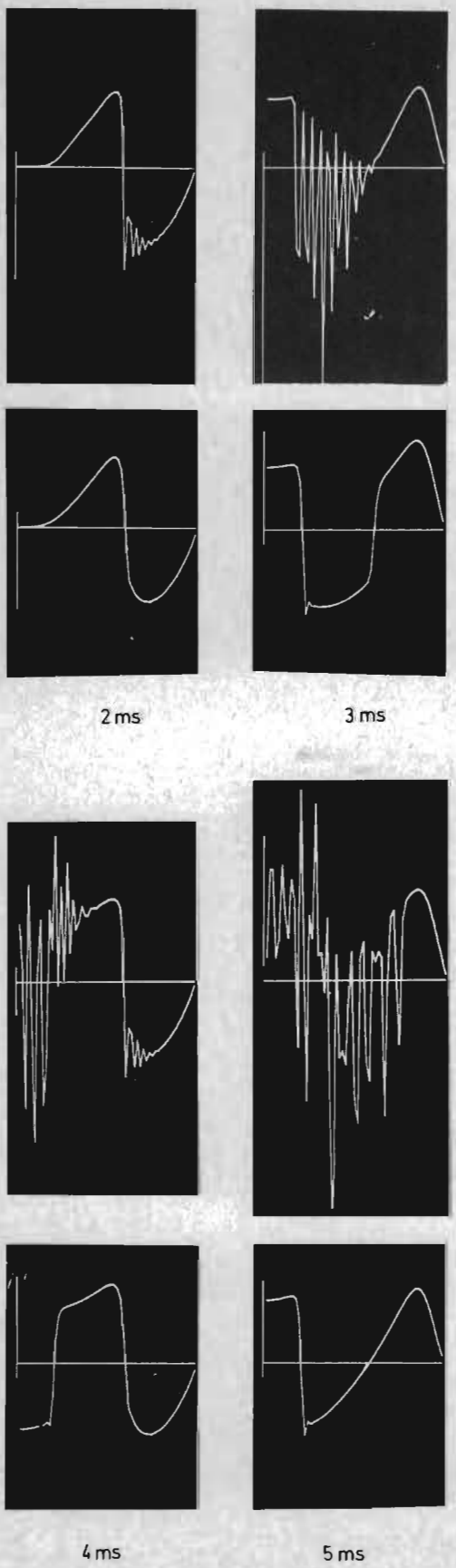

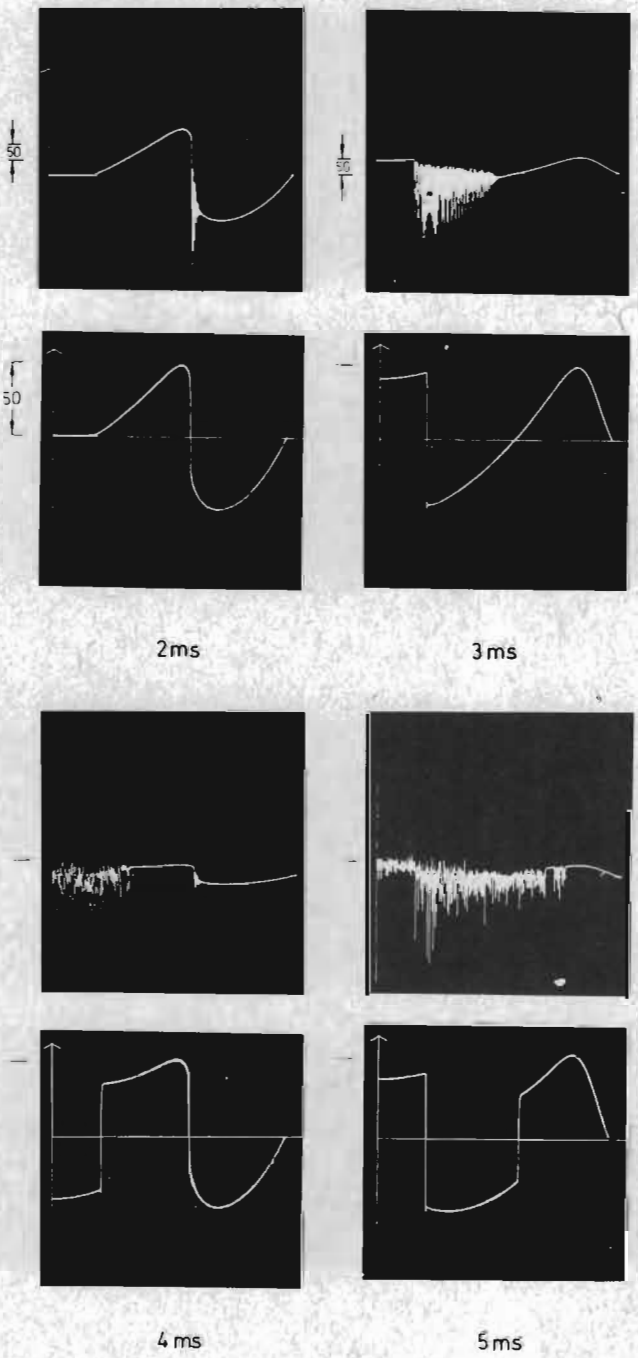

Fig 14 The same structure as Figure 13. The idealisation is now made with 600 element bars. The damping is 10^{-6}. It is interesting to note the influence of the fineness of the discretization. See (5)

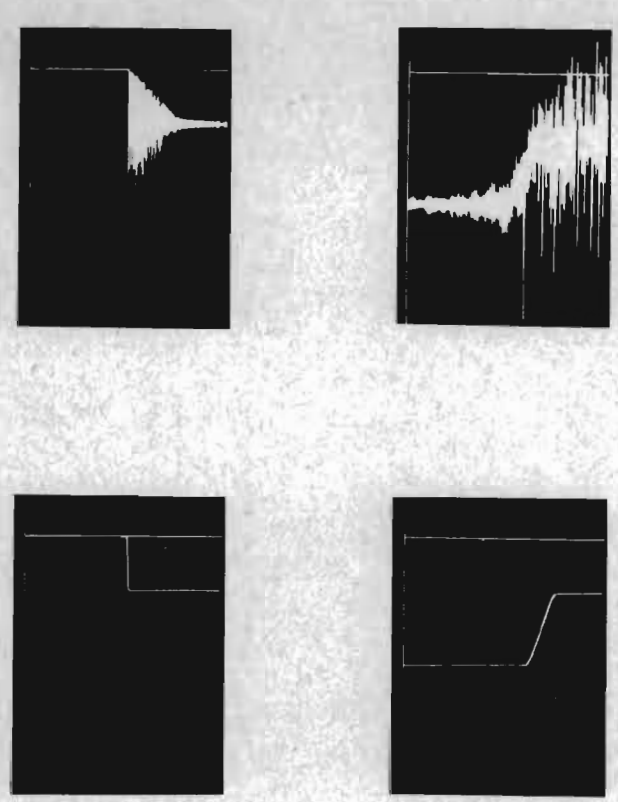

Fig 15 Mooney material 600 element bar
Compressive step load. Undamped and damped response at two different times.

III. Application of Large Step Algorithms

Because of the large step, direct solution (elimination, triangularisation or matrix inversion) of each time step is necessary.

Any linear vibrating system reduces to

$$M\ddot{r} + C\dot{r} + Kr = f \qquad (1)$$

and the algorithms of TABLE 2 lead to an equation of the form

$$D_1\begin{bmatrix} r_1 \\ \dot{r}_1 \end{bmatrix} = D_0\begin{bmatrix} r_0 \\ \dot{r}_0 \end{bmatrix} + F \qquad (2)$$

where D_0, D_1 and F are given in Figs. 16 and 17 for the 3rd and 5th degree algorithms.

Some applications are shown in the Figures 18 to 24. For other explanations the user should also consult the references.

Fig 16 Matrices for the first and second algorithms of resolution of equation (2)

$$D_1 = \begin{bmatrix} \left[M + \frac{\tau^2}{4}K\right] & \frac{\tau^2}{4}C \\ \frac{\tau}{2}K & \left[M + \frac{\tau}{2}C\right] \end{bmatrix}$$

$$D_0 = \begin{bmatrix} \left[M - \frac{\tau^2}{4}K\right] & \left[\tau M - \frac{\tau^2}{4}C\right] \\ -\frac{\tau}{2}K & \left[M - \frac{\tau}{2}C\right] \end{bmatrix}$$

$$F = \begin{bmatrix} \frac{\tau^2}{4}\left[f_0 + f_1\right] \\ \frac{\tau}{2}\left[f_0 + f_1\right] \end{bmatrix}$$

$n = 1, 2^{nd}$ Order Hermitian Polynomial of 1^{st} Degree (Newmark Algorithm)

$$D_1 = \begin{bmatrix} \left[M + \frac{\tau^2}{6}K + \frac{\tau^3}{24}CM^{-1}K\right] & \left[\frac{\tau^2}{6}C - \frac{\tau^3}{24}\left(K - CM^{-1}C\right)\right] \\ \left[\frac{\tau}{2}K + \frac{\tau^2}{12}CM^{-1}K\right] & \left[M + \frac{\tau}{2}C - \frac{\tau^2}{12}\left(K - CM^{-1}C\right)\right] \end{bmatrix}$$

$$D_0 = \begin{bmatrix} \left[M - \frac{\tau^2}{3}K + \frac{\tau^3}{24}CM^{-1}K\right] & \left[\tau M - \frac{\tau^2}{3}C - \frac{\tau^3}{24}\left(K - CM^{-1}C\right)\right] \\ \left[-\frac{\tau}{2}K + \frac{\tau^2}{12}CM^{-1}K\right] & \left[M - \frac{\tau}{2}C - \frac{\tau^2}{12}\left(K - CM^{-1}C\right)\right] \end{bmatrix}$$

$$F = \begin{bmatrix} \left[\frac{\tau^2}{3}I - \frac{\tau^3}{24}CM^{-1}\right] & \left[\frac{\tau^2}{6}I + \frac{\tau^3}{24}CM^{-1}\right] \\ \left[\frac{\tau}{2}I - \frac{\tau^2}{12}CM^{-1}\right] & \left[\frac{\tau}{2}I + \frac{\tau^2}{12}CM^{-1}\right] \end{bmatrix} \begin{bmatrix} f_0 \\ f_1 \end{bmatrix} + \begin{bmatrix} \frac{\tau^3}{24}\left(\dot{f}_0 - \dot{f}_1\right) \\ \frac{\tau^2}{12}\left(\dot{f}_0 - \dot{f}_1\right) \end{bmatrix}$$

$n = 2, 4^{th}$ Order Hermitian Polynomial of 3^{rd} Degree

$$D_1 = \begin{bmatrix} \left[M + \frac{3}{20}\tau^2 K + \frac{\tau^3}{24} CM^{-1}K - \frac{\tau^4}{240}\left(KM^{-1} - (CM^{-1})^2\right)K\right] & \left[\frac{3}{20}\tau^2 C - \frac{\tau^3}{24}\left(K - CM^{-1}C\right) - \frac{\tau^4}{240} KM^{-1}C\right] \\ \left[\frac{\tau}{2}K + \frac{\tau^2}{10} CM^{-1}K - \frac{\tau^3}{120}\left(KM^{-1} - (CM^{-1})^2\right)K\right] & \left[M + \frac{\tau}{2}C - \frac{\tau^2}{10}\left(K - CM^{-1}C\right) - \frac{\tau^3}{120}\left(CM^{-1}K + (KM^{-1} - (CM^{-1})^2)C\right)\right] \end{bmatrix}$$

$$D_0 = \begin{bmatrix} \left[M - \frac{7}{20}\tau^2 K + \frac{7}{120}\tau^3 CM^{-1}K + \frac{\tau^4}{240}\left(KM^{-1} - (CM^{-1})^2\right)K\right] & \left[\tau M - \frac{7}{20}\tau^2 C - \frac{7}{120}\tau^3\left(K - CM^{-1}C\right) + \frac{\tau^4}{240} KM^{-1}C\right] \\ \left[-\frac{\tau}{2}K + \frac{\tau^2}{10} CM^{-1}K + \frac{\tau^3}{120}\left(KM^{-1} - (CM^{-1})^2\right)K\right] & \left[M - \frac{\tau}{2}C - \frac{\tau^2}{10}\left(K - CM^{-1}C\right) + \frac{\tau^3}{120}\left(CM^{-1}K + (KM^{-1} - (CM^{-1})^2)C\right)\right] \end{bmatrix}$$

$$F = \begin{bmatrix} \left[\frac{7}{20}\tau^2 I - \frac{7}{120}\tau^3 CM^{-1} - \frac{\tau^4}{240}\left(KM^{-1} - (CM^{-1})^2\right)\right]\left[\frac{3}{20}\tau^2 I + \frac{\tau^3}{24} CM^{-1} - \frac{\tau^4}{240}\left(KM^{-1} - (CM^{-1})^2\right)\right] \\ \left[\frac{\tau}{2}I - \frac{\tau^2}{10}CM^{-1} - \frac{\tau^3}{120}KM^{-1} + \frac{\tau^3}{120}(CM^{-1})^2\right]\left[\frac{\tau}{2}I + \frac{\tau^2}{10}CM^{-1} - \frac{\tau^3}{120}\left(KM^{-1} - (CM^{-1})^2\right)\right] \end{bmatrix} \begin{bmatrix} r_0 \\ r_1 \end{bmatrix} \cdot \begin{bmatrix} \left[\frac{7}{120}\tau^3 I - \frac{\tau^4}{240} CM^{-1}\right]\left[-\frac{\tau^3}{24} I - \frac{\tau^4}{240} CM^{-1}\right] \\ \left[\frac{\tau^2}{10} I - \frac{\tau^3}{120} CM^{-1}\right]\left[-\frac{\tau^2}{10} I - \frac{\tau^3}{120} CM^{-1}\right] \end{bmatrix} \begin{bmatrix} \dot{r}_0 \\ \dot{r}_1 \end{bmatrix} \cdot \begin{bmatrix} \frac{\tau^4}{240}\left(\ddot{r}_0 - \ddot{r}_1\right) \\ \frac{\tau^3}{120}\left(\ddot{r}_0 - \ddot{r}_1\right) \end{bmatrix}$$

Fig 17 Matrices for the third Algorithm ($n = 3$ 6th order Hermitian Polynomial of 5th Degree)

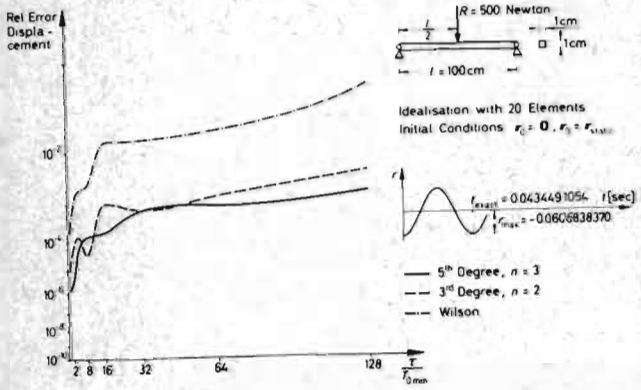

Fig 18 Free Oscillation of Beam

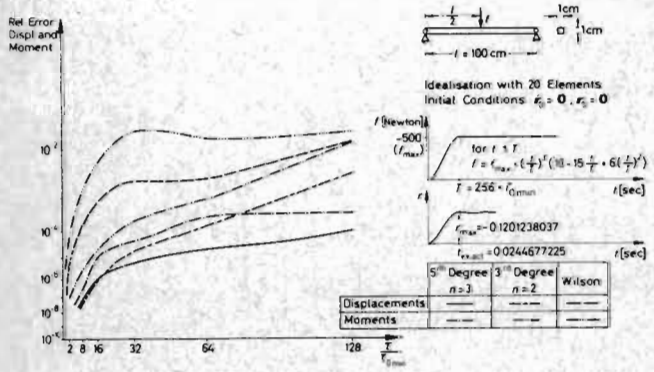

Fig 19 Forced Oscillation of Beam

Numerical Examples

In this section the new algorithms are applied to a number of linear problems and the results are compared with the well known Wilson method (6) with $\theta = 1{\cdot}4$ and in one case, with a modal analysis using the DYNAN package (7). The 'exact' solution in all problems is obtained by the third degree conditionally stable algorithm with a small time step.

Free vibration and dynamic loading of a beam

The dimensions of the beam which is divided into twenty consistant mass cubic finite elements are given in Figure 18. In the first example the beam is released from the static deflection due to a central load of 500 newtons. The solution is found with the stable algorithms ($n = 2$ and 3) and by the method of Wilson, using a time step ranging over $\tau / T_{0min} = 1, 2, 4, \ldots, 64, 128$. Note that the maximum time interval corresponds to almost exactly one-sixteenth of the fundamental period. In the curves of Figure 18 are shown the relative errors in the displacements at time corresponding to the maximum deflection of the 'exact' solution after one complete oscillation. The spectrum of the beam is very widely spaced and the contribution of the first mode to the initial static deflection is over 98 per cent of the total. Thus engineering accuracy is obtained by all methods. The small improvement of the fifth degree algorithm over the third degree is due to the better representation of the second and third modes. One sees that to achieve 0·1 per cent accuracy the integration step is respectively 2, 17, 75 T_{0min} for the Wilson, third degree and fifth degree algorithms.

In Figure 19 are presented the relative errors in the response of the beam to a 500 newton central load applied over a time of 256 as a fifth degree polynomial. The deflections and bending moments at the centre are compared at the time corresponding to the first maximum of the 'exact' solution. The maximum integration step is one half of the time of application of the load. The form of the load function is such that all methods integrate the total impulse.

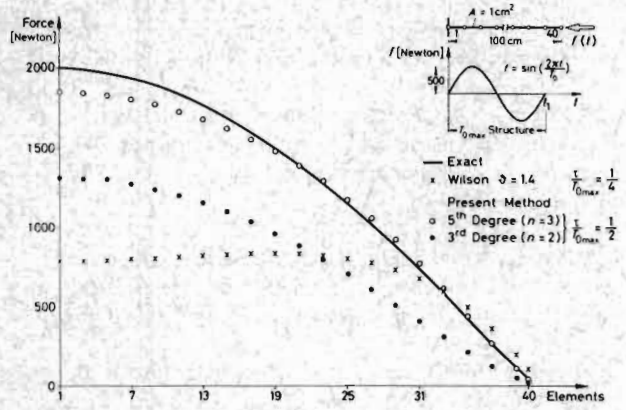

Fig 20 Force along length of Bar at =

Bar with resonant loading

The bar which is divided into 40 lumped mass elements is supported at one end and loaded with a sinusoidal force of amplitude 500 newtons and of period equal to the fundamental T_{omax}. In Figure 20 the force along the bar is shown after time of one period. The third and fifth degree algorithms are applied with a integration step of $\frac{1}{2} T_{omax}$ and the Wilson algorithm with $\tau = \frac{1}{4} T_{omax}$. Figure 21 shows the same example with the integration step of $\frac{1}{8} T_{omax}$ in all three methods. The increase in accuracy with the use of the higher order algorithms is much more evident than in the previous example because the modal frequencies are more closely spaced.

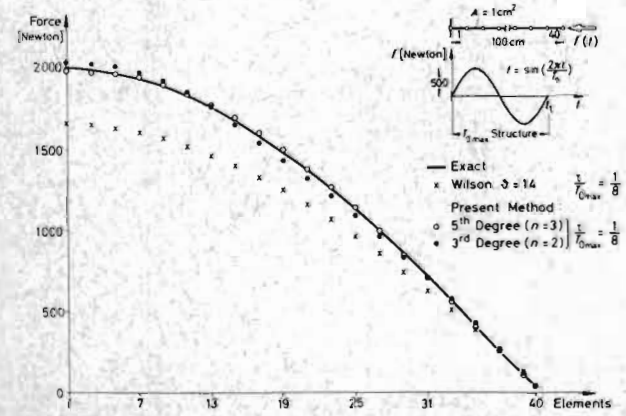

Fig 21 Force along length of Bar at = for a different time step.

Vibration of beam with damping

The damping matrix is taken as the sum of parts proportional to the stiffness and mass matrices. Thus

$$C = \bar{\alpha} M + \bar{\beta} K$$

where $\bar{\alpha} = 10$ and $\bar{\beta} = 10^{-5}$.

The beam is released from static equilibrium under a central load and in Figure 22 are plotted the errors in the deflection at the exact solution time of a complete oscillation.

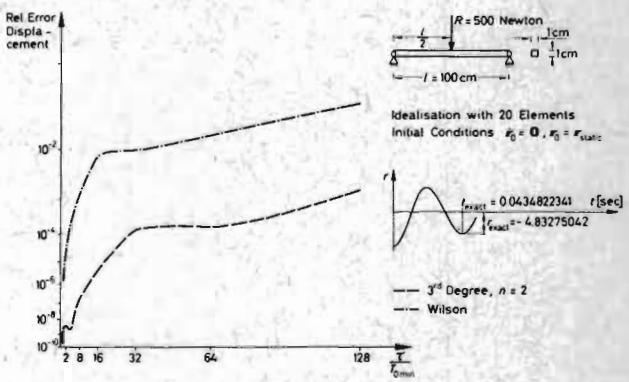

Fig 22 Damped Oscillation of Beam

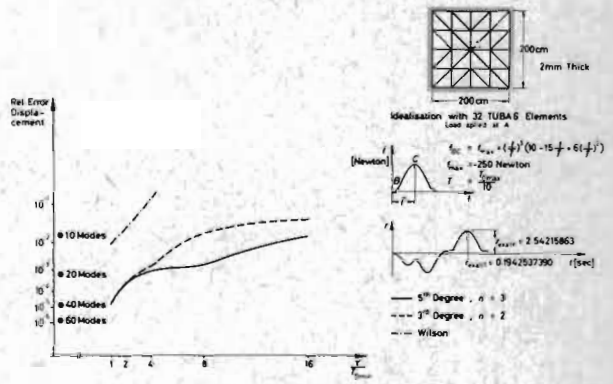

Fig 23 Forced Oscillation of a Square Clamped Plate

Clamped plate with central transient load

The plate whose dimensions are given in Figure 23 is idealized as 32 TUBA 6 finite elements. A central load is represented by two fifth degree polynomials applied over a total time of $T_{omax}/5$. The deflections at the centre are compared at the time of the first maximum defined in Figure 23. It will be noticed that the Wilson method gives 1 per cent error even when The same time step gives only 0·002 per cent error in the third degree algorithm ($n = 2$) and to reach 1 per cent error a time step of $7 T_{omin}$ is required. Also in the Figure are the errors of a modal analysis by the DYNAN method &5) using 10, 20, 40 and 60 modes of a total of 106 modes.

Flutter Problem

Another example studied with the 3rd order algorithm is the behaviour of a triangular plate immersed in a supersonic flow. The plate clamped at one of its edges is represented by a TUBA 6 finite element. The speed is sought for which the plate will start to flutter. Figure 24 shows that it will happen for a Mach number of 2.80. The sensibility of the vibration with the Mach number is clearly demonstrated by the curve obtained for a Mach number of 2.85 which gives rapid divergence. The study was made for different time steps. The curves are obtained for time step equal to about 1/25 of the resulting flutter period. For a time step 1/3 of this last period, the results were still useful from a practical point of view: for a Mach number equal to 2.80 it was possible to notice flutter; for 2.85 divergence.

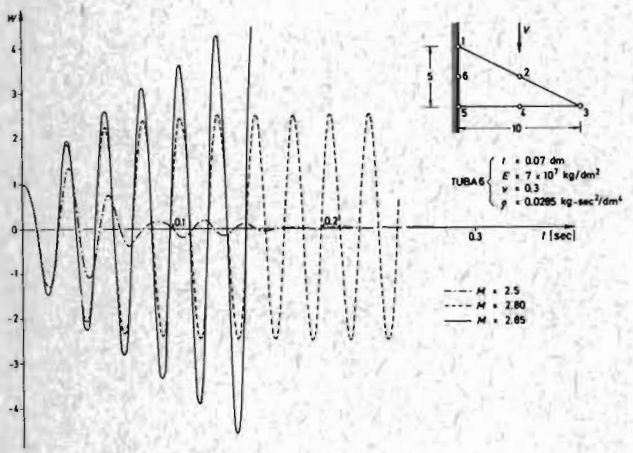

Fig 24 Flutter of a Plate. TUBA 6 finite element. Displacement of node 3 (in dm) as function of the time for different Mach numbers.

References

1 G.L. Goudreau and R.L. Taylor, Evaluation of numerical integration methods in elastodynamics, Computer Methods in Applied Mechanics and Engineering 2, No. 1, 65-68 (1972)

2 J.H. Argyris, P.C. Dunne and T. Angelopoulos, Non-linear oscillations using the finite element technique, Computer Methods in Applied Mechanics and Engineering, 2, 203-250 (1973)

3 J.H. Argyris, P.C. Dunne and T. Angelopoulos, Dynamic response by large step integration, Earthquake Engineering and Structural Dynamics, 2, No. 3 (1973)

4 J.H. Argyris and P.C. Dunne, Some contributions to non-linear mechanics, Colloque IRIA Versailles, Dec. 1973, (springer Verlag, Berlin (to be published)

5 J.H. Argyris, P.C. Dunne, T. Angelopoulos, B. Bichat, Large natural strains and some special difficulties due to non-linearity and incompressibility in finite elements Computer Methods in Applied Mechanics and Engineering (to be published)

6 E.L. Wilson, I. Farhoomand and K.J. Bathe, Non-linear dynamic analysis of complex structures, Int. J. Earthquake Engineering Struct. Dyn., 1, 241-252 (1973)

7 K.A. Braun, O.E. Brönlund, J. Bühlmeier, G. Dietrich, G. Frik, T.L. Johnsen, H.T. Kiesbauer, G.A. Malejannakis, K. Straub and G. Vallianos, DYNAN lecture notes with computation examples, ISD Report No. 109 University of Stuttgart (1971)